Journal of Infection and Public Health 19 (2026) 103162

Contents lists available at ScienceDirect

Journal of Infection and Public Health

journal homepage: www.elsevier.com/locate/jiph

Original article

# Distinct serum metabolic profiles with supportive diagnostic value in differentiating tuberculosis and *Mycobacterium avium* complex pulmonary disease

Keu Eun San Kim [a,1], Ye Jin Lee [b,1], Ji Hae Park [a], Nakwon Kwak [c], Su-Young Kim [d], Byung Woo Jhun [d], Jae-Joon Yim [c,e,*], Sung Jae Shin [a,**]

[a] Department of Microbiology, Institute for Immunology and Immunological Diseases, Graduate School of Medical Science, Brain Korea 21 Project, Yonsei University College of Medicine, Seoul, Republic of Korea
[b] Division of Pulmonary and Critical Care Medicine, Department of Internal Medicine, Seoul National University College of Medicine, Seoul National University Bundang Hospital, Seongnam, Republic of Korea
[c] Division of Pulmonary and Critical Care Medicine, Department of Internal Medicine, Seoul National University Hospital, Seoul, Republic of Korea
[d] Division of Pulmonary and Critical Care Medicine, Department of Medicine, Samsung Medical Center, Sungkyunkwan University School of Medicine, Seoul, Republic of Korea
[e] Department of Internal Medicine, Seoul National University College of Medicine, Seoul, Republic of Korea

ARTICLE INFO

*Article history:*
Received 12 September 2025
Received in revised form 20 January 2026
Accepted 25 January 2026

*Keywords:*
Differential diagnosis
Metabolomics
*Mycobacterium avium* complex
Nontuberculous mycobacteria
Tuberculosis

ABSTRACT

*Background:* Pulmonary infectious diseases caused by Mycobacterium species, including Mycobacterium tuberculosis and Mycobacterium avium complex (MAC), remain significant public health threats. However, current gold-standard diagnostics are time-consuming and have limited ability to differentiate these clinically similar presentations. This study investigated serum metabolic distinctions between tuberculosis (TB) and MAC pulmonary disease (MAC-PD) to identify biomarkers with supportive diagnostic value for differential diagnosis.

*Methods:* We performed LC/MS-based metabolic profiling of 181 serum samples from TB and MAC-PD patients. The study cohort was subsequently divided into a training set (TB, n = 30; MAC-PD, n = 30) and a validation set (TB, n = 51; MAC-PD, n = 70).

*Results:* Five key metabolites were identified, including four sphingoid base lipids that were decreased in TB compared with MAC-PD, and 2-hydroxyglutaric acid (2-HG), which was increased. Logistic regression using this five-metabolite panel achieved strong discriminatory performance, with an area under the curve of 0.988 (95 % CI: 0.970–1.000) in the training set and 0.997 (95 % CI: 0.991–1.000) in the validation set. Consistent performance across multiple machine learning models reinforces the stability and supportive diagnostic value of the five-metabolite panel.

*Conclusions:* This study provides a novel approach for the differential diagnosis of two major mycobacterial pulmonary diseases. The identified metabolites, particularly alterations in sphingoid base lipids and 2-HG, demonstrated robust discriminative potential. These findings support their potential role as biomarkers in clinical practice, enabling earlier and more accurate differentiation of TB and MAC-PD.



## Introduction

Pulmonary infectious diseases caused by *Mycobacterium* species remain a significant public health concern worldwide. According to the 2025 Global Tuberculosis Report from the World Health Organization, tuberculosis (TB) has regained its position as the leading cause of death from a single infectious agent, with 10.7 million new cases and 1.23 million deaths worldwide in 2024 [1]. In South Korea, TB continues to pose a major health burden, with the

* Corresponding author at: Department of Internal Medicine, Seoul National University College of Medicine, Seoul, Republic of Korea.
** Correspondence to: Department of Microbiology, Yonsei University College of Medicine, Seoul 03722, Republic of Korea.
*E-mail addresses:* yimjj@snu.ac.kr (J.-J. Yim), sjshin@yuhs.ac (S.J. Shin).
[1] These authors equally contributed to this study.

https://doi.org/10.1016/j.jiph.2026.103162

second-highest incidence rate (38 cases per 100,000) and the fifth-highest mortality rate (3 deaths per 100,000) among Organization for Economic Cooperation and Development member countries in 2023 [2].

Nontuberculous mycobacteria (NTM) are ubiquitous environmental organisms that cause opportunistic infections with diverse clinical phenotypes [3]. The incidence and prevalence of NTM pulmonary disease (PD) are rising globally, including in South Korea, where the annual prevalence increased from 11.4 to 56.7 cases per 100,000 population between 2010 and 2021 [4]. Among more than 200 NTM species, *Mycobacterium avium* complex (MAC), primarily *M. avium* and *M. intracellulare*, is the predominant cause, responsible for approximately 60–70 % of NTM infections globally [3,5]. In South Korea, MAC infections account for over 70 % of NTM cases and continue to rise [6].

The rising burden of TB and MAC-PD highlights their significance not only as clinical entities but also as major public health concerns. Timely and accurate diagnosis is essential to reduce transmission, minimize inappropriate antimicrobial use, and alleviate the burden on healthcare systems.

Clinically, the diagnosis of pulmonary TB and MAC-PD requires an integrated assessment of clinical manifestation, chest radiographic evaluation, and microbiological confirmation through acid-fast bacilli (AFB) staining and culture [7]. This gold-standard approach, which relies heavily on sputum specimens, is not only time-consuming, often taking several weeks for culture results, but also challenging in patients unable to produce sputum. While PCR-based molecular diagnostics, such as the Xpert MTB/RIF assay, offer rapid detection of *Mycobacterium tuberculosis* (Mtb), rare Xpert-positive results may still occur in patients who ultimately have NTM-PD, potentially leading to diagnostic confusion. These uncommon positive results are instead attributed to clinically recognized factors such as Mtb–NTM coinfection, laboratory contamination or carry-over, or the detection of residual Mtb DNA from prior disease [8,9]. Such diagnostic ambiguity often leads to the empirical initiation of anti-TB treatment, resulting in misdiagnosis and inappropriate or unnecessary treatment of patients with NTM-PD [10]. Therefore, an early and accurate differential diagnosis between TB and MAC-PD is crucial for initiating tailored treatment regimens.

Blood-based tests are less invasive, easier to obtain, and broadly applicable, making them an attractive platform for advanced analytic approaches such as metabolomics. Mass spectrometry (MS)-based metabolomics, which quantifies low-molecular-weight metabolites, enables the detection of subtle biochemical changes that reflect host-pathogen interactions and disease processes. This approach has been increasingly applied to infectious diseases, cancer, and metabolic disorders, providing insights into metabolic reprogramming in response to pathological changes [11]. Importantly, recent serum-based metabolomics studies have demonstrated that both TB and other mycobacterial pulmonary infections are associated with distinct metabolic signatures, including characteristic alterations in polar and lipid metabolites [12–14]. These findings support the rationale for investigating serum metabolic signatures as potential biomarkers for differentiating TB from MAC-PD.

Pulmonary mycobacterial infections generate a highly inflammatory and metabolically stressed microenvironment, characterized by hypoxia, acidic conditions, and altered mitochondrial function. Hypoxia-driven metabolic reprogramming can disrupt conventional TCA cycle flux and α-ketoglutarate-dependent pathways, leading to the accumulation of atypical metabolic intermediates and other markers of redox imbalance [15]. In parallel, infection-induced inflammation triggers extensive alteration of host lipid metabolism. Phospholipids and sphingolipids, which play central roles in membrane structure, immune signaling, and antimicrobial defense, are frequently perturbed during pulmonary infection [16,17]. Together, these hypoxia-associated metabolic shifts and infection-driven lipid alterations constitute a biological rationale for investigating serum metabolomic signatures that may differentiate TB and MAC-PD. Despite these advances, the metabolic distinctions between TB and MAC-PD remain poorly defined, and a systematic evaluation of serum metabolite profiles could provide valuable clues for improving differential diagnosis. Therefore, we applied serum metabolic profiling in patients with TB and MAC-PD to identify polar and lipid metabolites as potential biomarkers with supportive diagnostic value for differential diagnosis.

## Materials and methods

### *Sample collection*

A total of 99 diagnostic serum samples were collected from patients with culture-confirmed TB at Seoul National University Hospital between August 2011 and September 2013. Of these, 18 samples were excluded due to extra-pulmonary TB or revised diagnosis of NTM-PD. Additionally, 100 diagnostic serum samples were collected from MAC-PD patients who fulfilled the American Thoracic Society criteria for NTM-PD [18] at Samsung Medical Center between January 2017 and February 2019. All cases were confirmed by sputum culture and PCR-based molecular diagnosis. In total, 181 serum samples (TB, n = 81; MAC-PD, n = 100) were collected, and all patients were Korean. The samples were randomly divided into a training set (n = 60) and a validation set (n = 121) in Fig. 1. This retrospective study was approved by the Institutional Review Boards of both institutions (Seoul National University Hospital, IRB No. H-2509–085–1676; Samsung Medical Center, IRB No. SMC-2008–09–016). The requirement for written informed consent was waived, as the study used previously collected diagnostic serum samples from an established clinical cohort, involved no additional patient contact or intervention, and used fully de-identified data. All procedures were conducted in accordance with the principles of the Declaration of Helsinki. Blood samples from patients at both Seoul National University Hospital and Samsung Medical Center were collected following an identical standardized protocol. Venous blood was drawn, allowed to clot for 30 min at room temperature, and centrifuged at 1500 × g for 10 min. The resulting serum was aliquoted into polypropylene tubes and immediately stored at −80 °C until further metabolomic analysis. All procedures strictly adhered to institutional protocols harmonized across both centers.

### *Polar metabolite analysis*

For polar metabolite analysis, 10 µL of serum was extracted with 70 % acetonitrile containing isotope-labeled internal standards, following a modified protocol [19]. Detailed information on chemicals, isotope-labeled standards, and extraction procedures is provided in Supplementary Methods. Polar metabolite profiling was performed using high-performance liquid chromatography (HPLC; Agilent 1200 series, Agilent Technologies, Santa Clara, CA, USA) coupled with a triple quadrupole mass spectrometer (QQQ; API 4000, AB SCIEX, Framingham, MA, USA). Separation was achieved with a BEH Amide column (4.6 × 250 mm, 3.5 µm; Waters, Milford, MA, USA) for positive ion mode and a Luna PFP(2) column (2.0 × 150 mm, 3 µm; Phenomenex, Torrance, CA, USA) for negative ion mode. The mobile phase composition and gradient conditions are described in Table S1. Mass spectral data were acquired by scheduled multiple reaction monitoring and analyzed using Analyst software (SCIEX). Detailed MS/MS parameters are described in Supplementary Methods, and compound-specific information, including Q1/Q3 transitions, retention time, collision energy, and ionization mode, together with overall operating parameters, is summarized in Table S2. Reproducibility of extraction and detection was confirmed by total ion chromatograms from pooled quality control (QC) samples (Fig. S1).

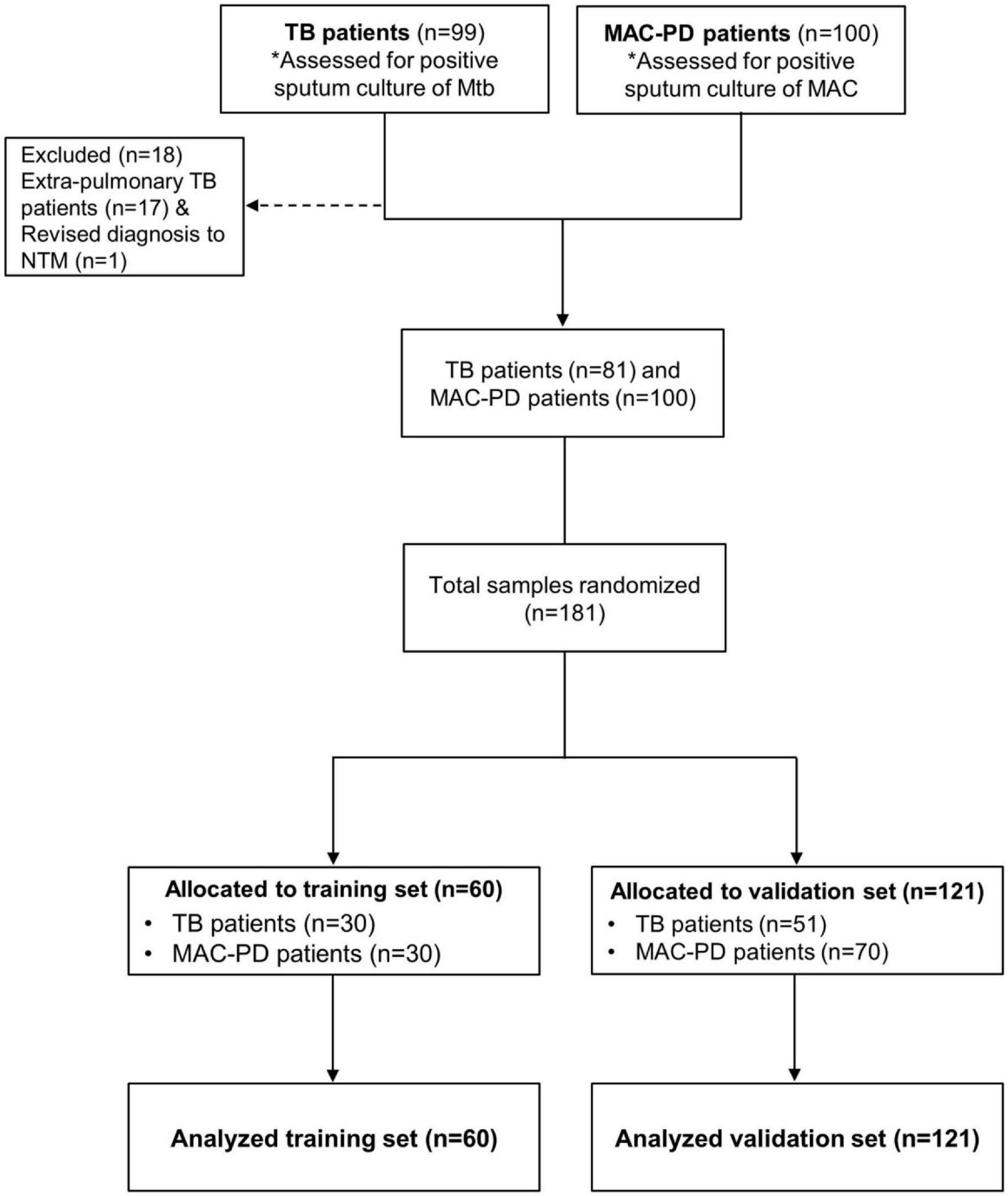


**Fig. 1.** Consort flow diagram of patients with TB and MAC-PD. Consort flow diagram illustrating the enrollment and allocation of TB and MAC-PD patients throughout the study. Participants were subsequently randomized into training and validation sets to explore the potential of serum metabolites as biomarkers with supportive diagnostic value for differentiating TB from MAC-PD. MAC-PD, *Mycobacterium avium* complex pulmonary disease; TB, tuberculosis.

*Lipid metabolite analysis*

For lipid metabolite analysis, 50 µL of serum was extracted with chloroform:methanol:water (2:1:1), and the lower phase was dried under nitrogen gas and reconstituted in isopropanol:acetonitrile:water (2:1:1) containing SPLASH LIPIDOMIX and Cer/Sph Mixture II (1:50) as internal standards, according to a modified method [20]. Detailed information on chemicals, isotope-labeled standards, and extraction procedures is provided in Supplementary Methods. Lipid metabolite profiling was conducted using an ultrahigh-performance liquid chromatography (UHPLC) system (UltiMate 3000; Thermo Fisher Scientific, Waltham, MA, USA) coupled with a Q Exactive Plus Orbitrap mass spectrometer (Thermo Fisher Scientific). Chromatographic separation was performed with a BEH C18 column (2.1 × 100 mm, 1.7 µm; Waters, Milford, MA, USA) under both positive and negative ion modes. Mobile phase composition and gradient conditions are provided in Table S3. Full-scan and data-dependent MS/MS spectra were acquired with high resolution and mass accuracy. Detailed MS/MS parameters are described in Supplementary Methods, and compound-specific information, including molecular weight, retention time, and ionization mode, is summarized in Table S4. Reproducibility was confirmed using pooled QC samples, as shown in Fig. S2.

*Data processing and metabolite identification* Putative metabolite identification was performed using a combination of exact mass, MS/MS fragmentation patterns, retention time, and comparison with in-

house and public databases. For polar metabolites, annotation was primarily supported by the Human Metabolome Database (HMDB, http://hmdb.ca) and literature searches. For lipid metabolites, raw spectral data were processed using Compound Discoverer 3.2 (Thermo Fisher Scientific), and annotations were further refined using HMDB, PubChem (http://pubchem.ncbi.nlm.nih.gov), and LIPID MAPS (http://lipidmaps.org), with consideration of accurate mass, retention time, and MS/MS spectral matching against in-house and public libraries.

*Statistical analysis*

All metabolite intensities were processed using QC-based normalization and log transformation. QC samples were injected at regular intervals to monitor analytical stability, and metabolites with a QC relative standard deviation (RSD) > 30 % were excluded. All samples were analyzed in a fully randomized injection order to minimize run-order effects.

Normalized metabolite levels were compared between TB and MAC-PD using an unpaired *t*-test or Mann-Whitney *U* test, as appropriate. Categorical variables were analyzed using the chi-square test. False discovery rate (FDR) correction was applied using the Benjamini-Hochberg procedure (FDR-adjusted p-value < 0.05). All statistical analyses were performed with IBM Statistical Package for Social Sciences (SPSS), version 28.0.0 (IBM Corp., Armonk, NY, USA).

For model development and evaluation, the dataset was randomly divided into a training set (~30 %) and an independent validation set (~70 %). Although this split ratio is not conventional, a larger validation set allowed a more stringent and conservative assessment of the discriminatory diagnostic performance of the selected metabolites and helped reduce the likelihood of overfitting.

For multivariate analysis, partial least-squares discriminant analysis (PLS-DA) was performed. Metabolites with a variable importance in projection (VIP) score > 1.2 were identified in MetaboAnalyst 6.0 (http://metaboanalyst.ca). Data visualization, including volcano plots, bar plots, and scatter plots, was performed using Prism 9.0.2 (GraphPad, San Diego, CA, USA), and chord diagrams were generated using Origin (OriginLab, Northampton, MA, USA).

Diagnostic performance was further assessed using univariate and multivariate receiver operating characteristic (ROC) analyses. Logistic regression, random forest, support vector machine (SVM) with a radial basis function (RBF) kernel, neural network, and XGBoost models were trained on the training set with 10-fold cross-validation to optimize internal parameters, and their final performance was evaluated on the validation set. Cross-validated area under the curve (AUC), with 95 % confidence intervals (CI), was computed from out-of-fold predictions. All multivariate analyses were performed in R software, version 4.3.3 (R Foundation for Statistical Computing, Vienna, Austria).

To assess whether demographic differences influenced metabolite-disease associations, additional logistic regression analyses were performed with TB and MAC-PD as the outcome. Each metabolite was modeled separately with adjustment for age, sex, and smoking. Adjusted odds ratios with 95 % CI were reported in Table S5.

## Results

*Baseline characteristics*

The baseline characteristics of the study population are summarized in Table 1. A total of 81 TB patients (30 in the training set and 51 in the validation set) and 100 MAC-PD patients (30 in the training set and 70 in the validation set) were included. In the training set, MAC-PD patients were significantly older than TB patients (median age: 58 vs. 50 years in the training set, p-value = 0.020), whereas no significant age difference was observed in the validation set (59 vs. 58 years, p-value = 0.304). Body mass index was lower in MAC-PD than in TB patients in the training set (20.9 vs. 21.8 kg/m², p-value = 0.014), although the difference was not significant in the validation set (p-value = 0.298). Sex distribution showed a consistent difference, with females predominating in the MAC-PD group (83 % vs. 43 % in the training set; 79 % vs. 37 % in the validation set, both p-value < 0.001). Smoking status also differed, with never-smokers more frequent among MAC-PD patients (86.7 % vs. 66.7 % in the training set, $P = 0.070$; 82.9 % vs. 53 % in the validation set, p-value < 0.001). Sputum smear positivity was more common in TB patients in the training set (26.7 % vs. 10 %), although not statistically significant (p-value = 0.16), whereas in the validation set, smear positivity was higher in MAC-PD (42.9 % vs. 23.5 %, $P = 0.027$). Radiologic findings showed no significant difference in the presence of cavitary lesions between the two groups in either set (p-value > 0.390 and p-value > 0.231, respectively). As expected, all TB cases were caused by *M. tuberculosis*. Among MAC-PD patients, *M. avium* and *M. intracellulare* accounted for 37 % and 63 % of cases in the training set, and 50 % each in the validation set. Given the distinct epidemiological profiles of TB and MAC-PD, differences in baseline characteristics such as age, sex, and smoking status were expected and may contribute to metabolic variability. To minimize potential confounding, subgroup analyses stratified by these variables were also performed.

*Comparative serum metabolic profiling of TB and MAC-PD*

Metabolomics analysis was conducted using 181 serum samples to explore potential biomarkers with supportive diagnostic value for differentiating TB from MAC-PD. Samples were randomly divided into a training set (TB, n = 30; MAC-PD, n = 30) for initial screening and a validation set (TB, n = 51; MAC-PD, n = 70) for subsequent confirmation of candidate metabolites. A total of 146 polar metabolites were detected using HPLC-QQQ/MS, and 3184 lipid metabolites were detected using UHPLC-Q-Exactive Orbitrap/MS. PLS-DA revealed a tendency toward clear separation between TB and MAC-PD patients in both the training and validation sets. The PLS-DA models achieved cross-validated classification accuracies of 0.983 in the training set and 0.992 in the validation set, with corresponding $R^2Y$ values of 0.741 and 0.880 and $Q^2$ values of 0.764 and 0.813, respectively **(**Fig. 2**A and B)**. Key metabolites contributing to group separation were ranked by VIP scores > 1.2, a commonly applied threshold in metabolomic studies. The top 20 variables from both the training and validation sets were presented to evaluate their relative contributions to the PLS-DA models **(**Fig. 2**C and D)**. Volcano plots were generated separately for the training and validation sets, highlighting discriminative metabolites with $|\log_2 FC| > 0.26$ (corresponding to fold change ≥ 1.2 or ≤ 0.8) and adj p-value < 0.05 as significant **(**Fig. 2**E and F)**. Among these, five metabolites were consistently identified across both sets as a robust marker for differential diagnosis: four sphingoid base lipids ($\log_2 FC < -0.7$, adj p-value < 0.001) and 2-hydroxyglutaric acid (2-HG), which exhibited the strongest statistical association ($\log_2 FC > 2$, adj p-value < 0.001).

*Consistent metabolites for differential diagnosis between TB and MAC-PD in the training and validation sets*

Metabolic profiles were screened using predefined cut-off criteria (VIP > 1.2, $|\log_2 FC| > 0.26$, and adj p-value < 0.05). A total of 63 metabolites in the training set and 52 in the validation set significantly discriminated between TB and MAC-PD patients **(**Tables S6 and S7**)**. The overall patterns of metabolic profiling were largely consistent across sets: TB patients exhibited lower levels of sphingomyelin (SM), ceramide (Cer), phosphatidylcholine (PC), phosphatidylethanolamine (PE), and other lipid species, while showing

**Table 1**
Characteristics of the study population with TB and MAC-PD patients.

| Characteristics | Training set | | | Validation set | | |
|---|---|---|---|---|---|---|
| | TB | MAC-PD | p-value | TB | MAC-PD | p-value |
| Subjects | 30 | 30 | | 51 | 70 | |
| Age, years | 50 (34–64) | 58 (52–62) | 0.020[a] | 58 (42–67) | 59 (53–65) | 0.304[b] |
| BMI, kg/m | 21.8 (20.9–23.6) | 20.9 (19–21.4) | 0.014[a] | 21 (19.4–22.3) | 20.9 (18.6–21.7) | 0.298[a] |
| Never Smoker | 20 (66.7) | 26 (86.7) | 0.070[c] | 27 (53) | 58 (82.9) | < 0.001[c] |
| AFB Smear | 8 (26.7) | 3 (10) | 0.160[c] | 12 (23.5) | 30 (42.9) | 0.027[c] |
| Sex | | | 0.001[c] | | | < 0.001[c] |
| Male | 17 (56.7) | 5 (16.7) | | 32 (62.7) | 15 (21.4) | |
| Female | 13 (43.3) | 25 (83.3) | | 19 (37.3) | 55 (78.6) | |
| Etiologic organism | | | < 0.001[c] | | | < 0.001[c] |
| *M. tuberculosis* | 30 (100) | | | 51 (100) | | |
| *M. avium* complex | | 30 (100) | | | 70 (100) | |
| *M. avium* | | 11 (36.7) | | | 35 (50) | |
| *M. intracellulare* | | 19 (63.3) | | | 35 (50) | |
| Presence of cavitary | 10 (33.3) | 7 (23.3) | 0.390[c] | 15 (29.4) | 14 (20) | 0.231[c] |

Data are presented as number (percentage) or median (interquartile range).
AFB, acid-fast bacilli; BMI, body mass index; MAC-PD, *Mycobacterium avium* complex pulmonary disease; TB, tuberculosis.
[a] Unpaired *t*-test.
[b] Mann-Whitney *U* test.
[c] Chi-square test.

higher levels of polar metabolites and lysophosphatidylcholine (LPC) compared to MAC-PD patients (Fig. 3**A and B**).

Through statistical analysis, a total of 42 metabolites (12 polar and 30 lipid metabolites) were consistently identified in both sets as significant contributors (Fig. 4**A and** Fig. S3). For example, glucose 6-phosphate (G6-P), multiple sphingolipid species with combined chain lengths of 40–42, PCs with chain lengths of 30–40, and PEs with chain lengths of 36–40 were notably lower in TB patients. In contrast, 11 polar metabolites, including 2-HG, lactate, alanine, adenosine triphosphate (ATP), and choline, along with several LPC species with chain lengths of 16–18, were significantly elevated (Fig. 4**B and C**).

Together, these findings indicate that both global metabolic patterns and a consistently identified subset of 42 metabolites can effectively distinguish TB from MAC-PD, underscoring their potential diagnostic utility. To further evaluate this subset, we assessed their diagnostic performance using ROC analysis. Applying an AUC threshold greater than 0.90 prioritized five metabolites as the most discriminative: sphingosine (SPH, d16:1 and d18:1), sphinganine (SPG, d18:0), dimethylsphingosine (DMS, d18:1), and 2-HG (Fig. 5**A and** Table 2). We then examined their statistical characteristics to confirm robustness. All five metabolites exhibited strong contributions to group separation, with VIP scores > 2.3 in both sets. In the training set, VIP values ranged from 2.37 for 2-HG to 3.03 for DMS (d18:1), while in the validation set they ranged from 3.03 for 2-HG to 3.66 for DMS (d18:1). Directionality of changes was consistent across both sets: 2-HG was markedly elevated in TB compared to MAC-PD patients ($\log_2$ FC = 2.38 in the training set, 2.02 in the validation set; both adj p-value < 0.001), whereas SPH (d16:1 and d18:1), SPG (d18:0), and DMS (d18:1) were significantly reduced in TB ($\log_2$ FC ranging from −0.64 to −0.80; both adj p-value < 0.001).

In addition, subgroup analyses stratified by age, sex, and smoking status consistently identified the same five discriminatory metabolites as in the overall dataset, further supporting the robustness of our findings (Fig. S4). Moreover, all five metabolites remained significant predictors of TB and MAC-PD after adjustment for age, sex, and smoking in covariate-adjusted logistic regression models, indicating that demographic differences did not account for the observed metabolic patterns (Table S5). Finally, a chord diagram provided a visual summary of these alterations, highlighting their reproducible directionality across both sets and reinforcing the stability of this five-metabolite panel in differentiating TB from MAC-PD (Fig. S5).

*Optimal serum metabolite combinations for differential diagnosis between TB and MAC-PD*

We developed a predictive model integrating the five discriminatory metabolites. Logistic regression analysis demonstrated excellent diagnostic performance, with an AUC of 0.988 (95 % CI: 0.970–1.000) in the training set and 0.997 (95 % CI: 0.991–1.000) in the validation set. Model performance was further evaluated using several machine-learning approaches, including random forest, support vector machine (SVM) with a radial basis function (RBF) kernel, neural network, and XGBoost. These models yielded similarly high AUC values in both data sets (Fig. 5**B and** Table S8).

To examine whether these results reflected overfitting, we compared performance between training and validation sets and additionally applied 10-fold cross-validation. The validation AUCs were comparable to those of the training set, and cross-validation demonstrated stable performance across all classification methods (Table S8). In addition, each of the five metabolites showed strong individual discriminatory ability (AUC, 0.920–0.982; Table 2), indicating that high discriminative performance was observed not only at the multivariate level but also for individual metabolites.

## Discussion

Accurate differentiation between TB and NTM-PD remains a major clinical challenge, especially given the increasing global burden of NTM-PD. The current diagnostic pathway consists of AFB staining, culture-based microbiological confirmation, and radiographic evaluation, but each of these methods has important limitations. Although culture remains the gold standard, it typically requires 2–6 weeks to yield results, which delays appropriate therapy for TB, a transmissible disease requiring urgent treatment [21]. In addition, AFB staining cannot distinguish between Mtb and NTM [22], and radiographic findings often lack specificity. Several alternative approaches have been investigated to overcome these delays, including sputum-derived molecular assays, urinary metabolite signatures, and more recently, serum proteomic biomarkers [23–25]. These investigations underscore the need for faster and more broadly accessible diagnostic tools that are less dependent on specimen type and do not require prolonged culture-based workflows. However, despite these advances, serum-based metabolomic profiling has rarely been explored in this context. By identifying a small-molecule serum biomarker panel capable of discriminating TB

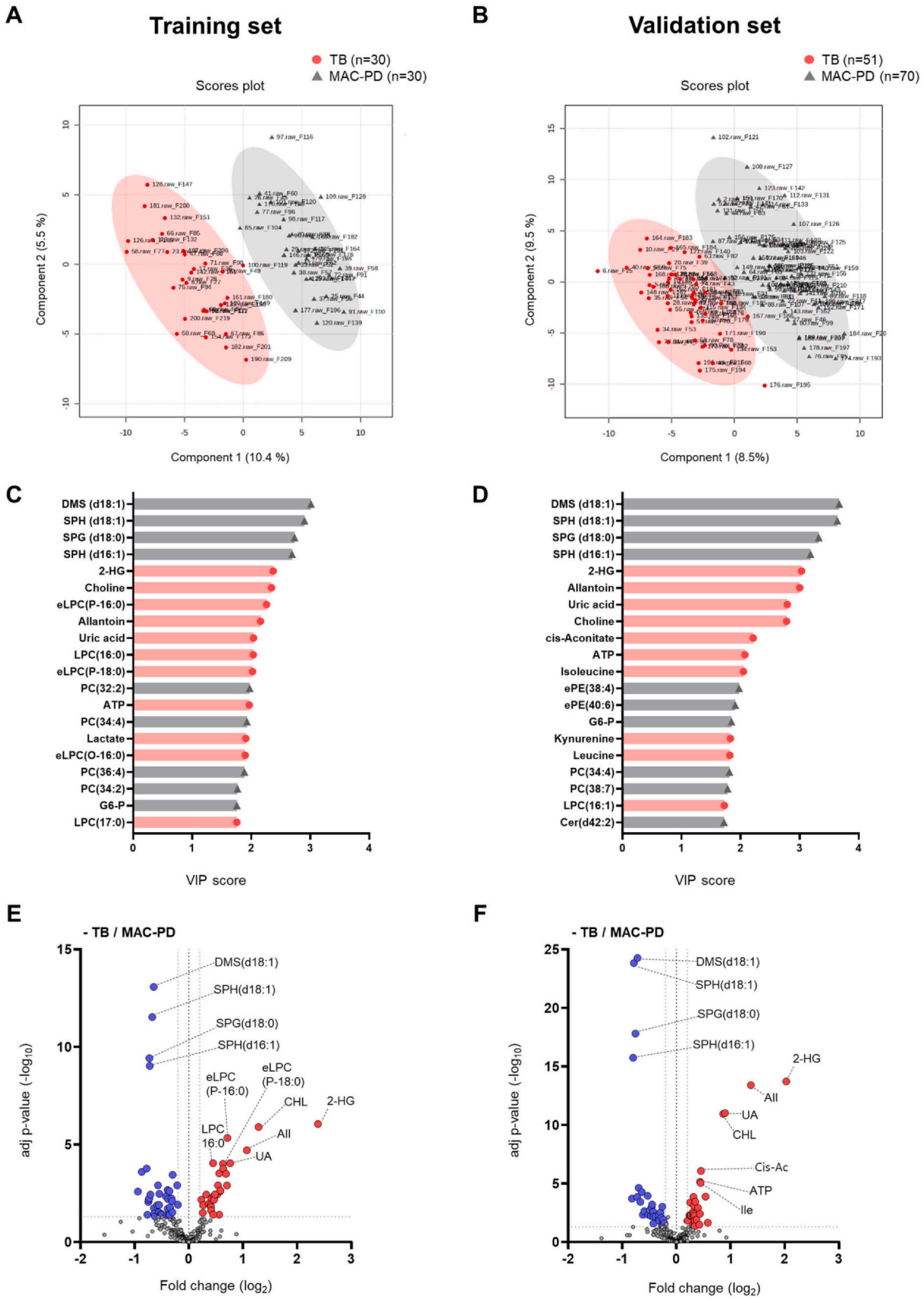


(caption on next page)

**Fig. 2.** Comparative analysis of serum metabolic profiling between TB and MAC-PD. PLS-DA score plots and VIP scores (top 20) derived from the (A and C) training and (B and D) validation sets, showing clear separation between TB (red) and MAC-PD (gray) patients. (E and F) Volcano plots display significantly different serum metabolite levels between the two groups. Only metabolites meeting the most stringent statistical criteria (adj p-value < 0.001 and VIP score > 2.0) are labeled to highlight the most robust candidates, including four sphingoid base lipids and 2-HG. Vertical lines indicate $|\log_2 FC| > 0.26$ (corresponding to fold change ≥ 1.2 or ≤ 0.8), and the horizontal line represents $-\log_{10}$ (adj p-value) > 1.3. Dots are colored red and blue to denote upregulated and downregulated metabolites, respectively. 2-HG, 2-hydroxyglutaric acid; All, allantoin; ATP, adenosine triphosphate; Cer, ceramide; CHL, choline; Cis-Ac, cis-aconitate; DMS, dimethylsphingosine; eLPC, ether lyso-phosphatidylcholine; ePE, ether phosphatidylethanolamine; FC, fold change; G6-P, glucose 6-phosphate; Ile, isoleucine; LPC, lyso-phosphatidylcholine; MAC-PD, *Mycobacterium avium* complex pulmonary disease; PC, phosphatidylcholine; PE, phosphatidylethanolamine; PLS-DA, partial least-squares discriminant analysis; SPG, sphinganine; SPH, sphingosine; TB, tuberculosis; VIP, variable importance in the projection.

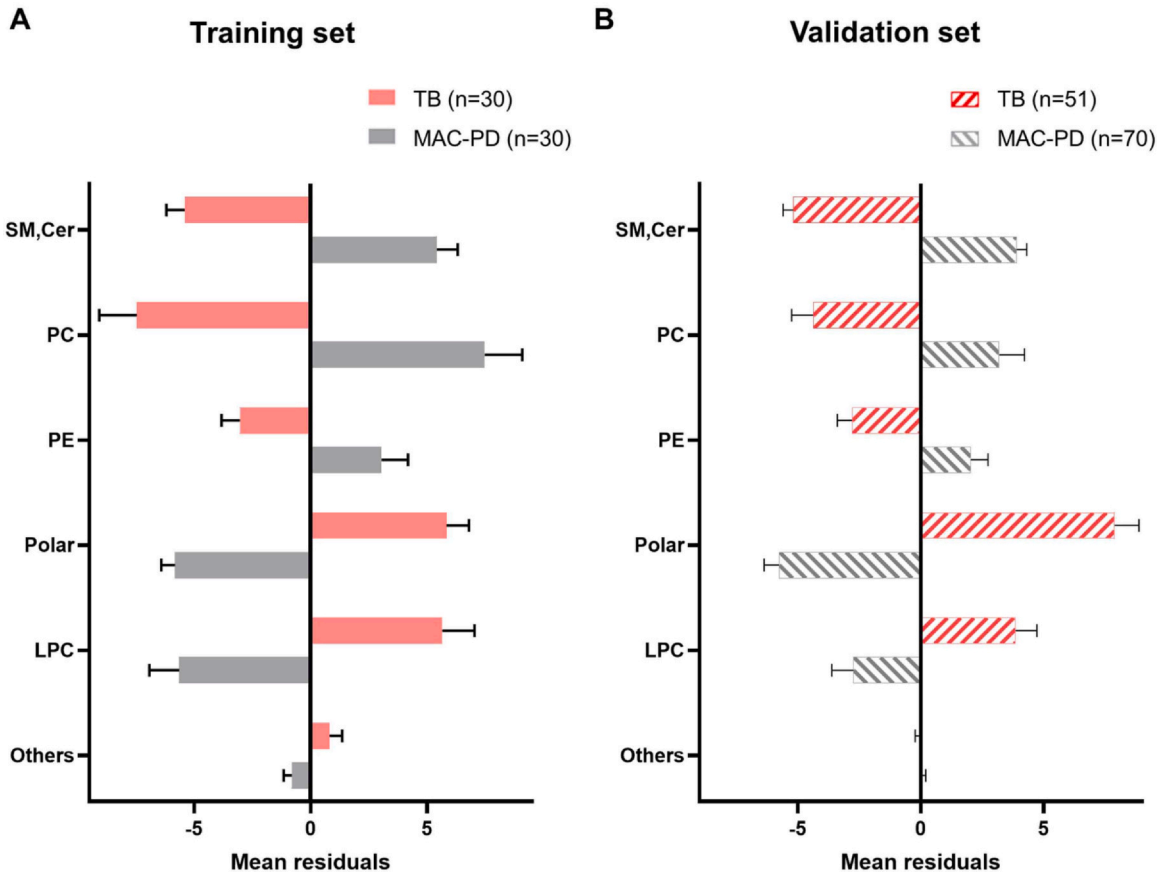


**Fig. 3.** Distinct serum metabolic differences across metabolite species differentiating TB and MAC-PD. (A and B) Bar plots show the baseline levels (mean ± standard error) of metabolite species that significantly differed between TB (red, red-pattern) and MAC-PD (gray, gray-pattern) patients in both the training and validation sets. The x-axes represent mean residuals, calculated as the sum of normalized residuals for individual metabolites within each species. These profiles highlight consistent metabolic trends distinguishing the two major mycobacterial pulmonary disease. MAC-PD, *Mycobacterium avium* complex pulmonary disease; TB, tuberculosis.

from MAC-PD, our study introduces a minimally invasive, rapidly measurable, and broadly implementable supportive diagnostic approach that can be readily integrated into routine clinical workflows.

Within this context, we applied serum metabolic profiling and identified distinct alterations in polar metabolites, phospholipids, and sphingolipids that consistently discriminated TB from MAC-PD. These results support the potential of blood-based metabolomics as a complementary tool to conventional microbiological assays and highlight underlying immunometabolic differences between the two major mycobacterial pulmonary diseases. In general, immune cells shift from oxidative phosphorylation to glycolysis upon stimulation by microbial ligands or pro-inflammatory cytokines [26]. This glycolytic switch, resembling the Warburg effect, is characterized by enhanced glucose uptake, accelerated glycolytic flux, and activation of the pentose phosphate pathway [27,28]. Hypoxia-inducible factor-1α (HIF-1α) functions as a master regulator of this process, and its induction of IL-1β is critical for controlling Mtb and other bacterial infections [29]. Consistent with this paradigm, TB patients showed relatively lower serum G6-P and higher lactate, alanine, and ATP levels compared with MAC-PD patients. These findings suggest host-driven metabolic reprogramming toward glycolysis, reflecting adaptation to the hypoxic and inflammatory milieu that is more pronounced in TB than in MAC-PD. We also observed elevated serum levels of 2-HG, a metabolite strongly associated with hypoxia and acidic microenvironments. In cancer, 2-HG typically accumulates due to neomorphic IDH1/2 mutations that convert α-ketoglutarate to 2-HG [30,31]. In our study, TB patients showed a selective increase in 2-HG compared with MAC-PD patients, whereas isocitrate and α-ketoglutarate levels remained unchanged. Although serum metabolomics cannot fully capture the complexity of pulmonary infection, this is consistent with the presence of a hypoxic and acidic inflammatory milieu in TB and highlights a metabolic difference relative to MAC-PD.

Lipid metabolism was also differentially perturbed, with the most striking alterations observed in sphingolipids. SPH and SPG, the backbones of sphingolipids, function not only as membrane constituents but also as innate antimicrobial lipids and precursors of phosphorylated signaling molecules [32,33]. Previous studies have associated reduced sphingolipid levels with chronic infection or impaired ceramidase activity [34]. In line with these observations, our study demonstrated systemic depletion of sphingoid base lipids, including SPH (d16:1 and d18:1), SPG (d18:0), and DMS (d18:1), in

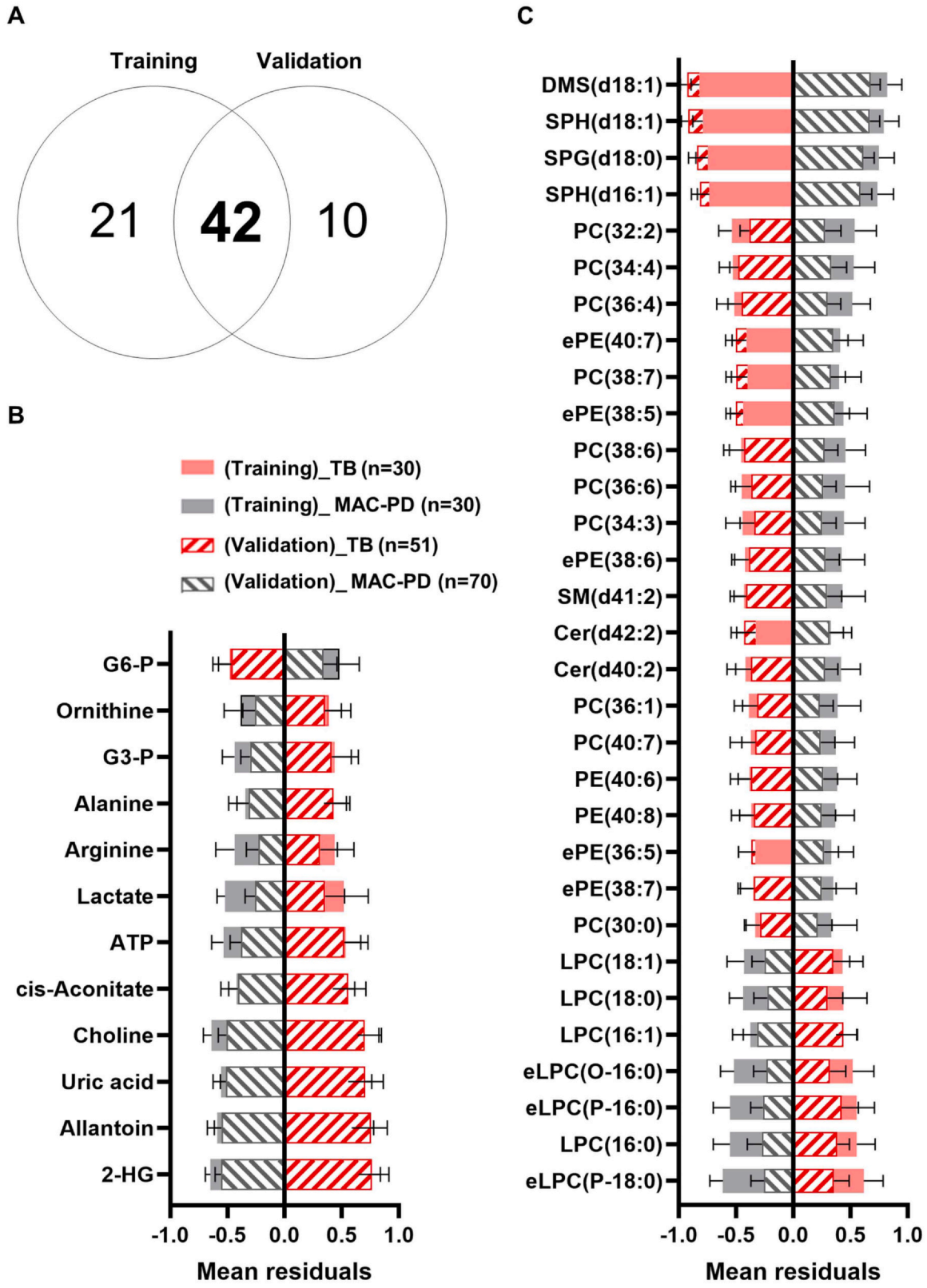


**Fig. 4.** Consistently identified metabolites with differential diagnostic value between TB and MAC-PD. (A) Venn diagram showing the number of discriminative metabolites identified in each subset: 63 in the training set and 52 in the validation set, with 42 overlapping metabolites consistently distinguishing TB from MAC-PD. Bar plots represent baseline levels (mean ± standard error of residuals) for the 42 shared metabolites, (B) including 12 polar metabolites and (C) 30 lipid metabolites. Colors indicate relative abundance in TB (red for training, red-pattern for validation) and MAC-PD patients (gray for training, gray-pattern for validation). The x-axes represent mean residuals, calculated for each metabolite. 2-HG, 2-hydroxyglutaric acid; ATP, adenosine triphosphate; Cer, ceramide; DMS, dimethylsphingosine; eLPC, ether lyso-phosphatidylcholine; ePE, ether phosphatidylethanolamine; G3-P, glycerol 3-phosphate; G6-P, glucose 6-phosphate; LPC, lyso-phosphatidylcholine; MAC-PD, *Mycobacterium avium* complex pulmonary disease; PC, phosphatidylcholine; PE, phosphatidylethanolamine; SM, sphingomyelin; SPG, sphinganine; SPH, sphingosine; TB, tuberculosis.

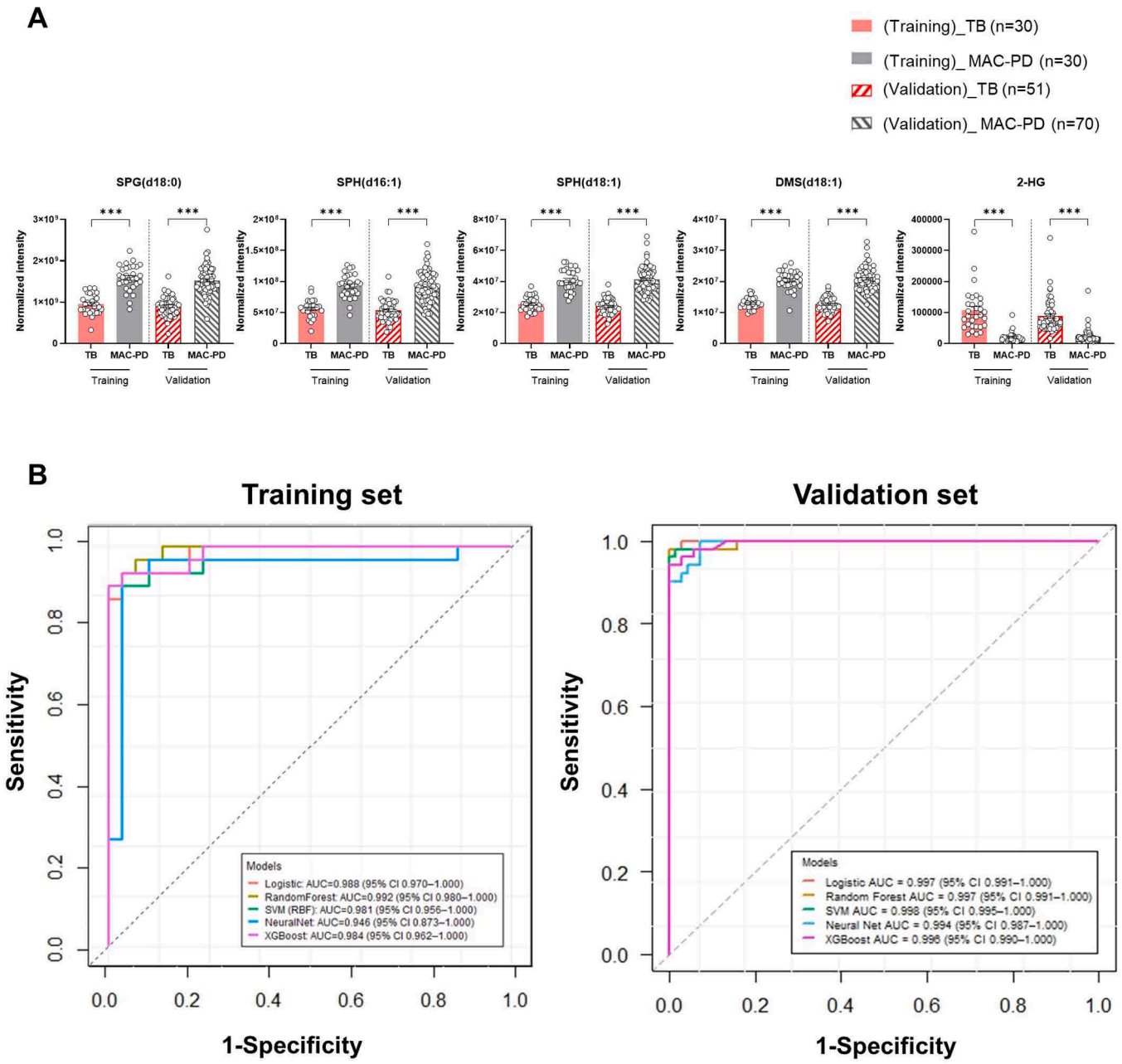


**Fig. 5.** Diagnostic performance of selected metabolites for differentiating TB from MAC-PD. (A) Serum levels of five metabolites (SPH (d16:1 and d18:1), SPG (d18:0), DMS (d18:1), and 2-HG) in patients with TB and MAC-PD across training and validation sets. (B) Multivariate machine learning-based ROC curve analyses of the five-metabolite panel in the training and validation sets. *Significance levels are indicated as FDR-adjusted * p-value < 0.05, ** p-value < 0.01, *** p-value < 0.001. 2-HG, 2-hydroxyglutaric acid; AUC, area under the curve; CI, confidence intervals; DMS, dimethylsphingosine; FDR, false discovery rate; MAC-PD, *Mycobacterium avium* complex pulmonary disease; ROC, receiver operating characteristic; SPG, sphinganine; SPH, sphingosine; TB, tuberculosis.

**Table 2**
ROC curve analysis in the training and validation sets.

| | Training set | | | Validation set | | |
|---|---|---|---|---|---|---|
| **Variable** | **AUC** | **SE**[a] | **95 % CI**[b] | **AUC** | **SE**[a] | **95 % CI**[b] |
| SPH (d16:1) | 0.933 | 0.035 | 0.856–0.991 | 0.920 | 0.025 | 0.862–0.963 |
| SPG (d18:0) | 0.940 | 0.029 | 0.876–0.988 | 0.945 | 0.021 | 0.897–0.981 |
| SPH (d18:1) | 0.970 | 0.017 | 0.927–0.996 | 0.979 | 0.010 | 0.955–0.995 |
| DMS (d18:1) | 0.964 | 0.030 | 0.888–1.000 | 0.982 | 0.009 | 0.960–0.998 |
| 2-HG | 0.973 | 0.019 | 0.930–1.000 | 0.963 | 0.018 | 0.922–0.995 |

2-HG, 2-hydroxyglutaric acid; AUC, area under the curve; DMS, dimethylsphingosine; ROC, receiver operating characteristic; SPG, sphinganine; SPH, sphingosine.
[a] SE: Standard error.
[b] 95 % CI: 95 % confidence interval calculated using the Binomial exact.

TB patients compared with those with MAC-PD. This relative depletion may compromise lipid-mediated antimicrobial defense and exacerbate inflammatory responses, potentially contributing to the distinct immunopathological features of TB compared to MAC-PD.

In addition to sphingolipids, phospholipid remodeling was also evident. Compared with MAC-PD patients, those with TB exhibited pronounced reductions in PC and PE, accompanied by an increase in LPC, a pro-inflammatory mediator generated by phospholipase-dependent remodeling [35,36]. Given that PC and PE are major surfactant phospholipids essential for pulmonary integrity [37–39], their depletion together with LPC accumulation suggests inflammation-driven remodeling that may impair surfactant function and compromise host defense. These findings are consistent with previous lipidomic studies in TB, which identified disrupted

phospholipid turnover as a hallmark of TB-associated inflammation [40–42].

Although the multivariate models produced very high AUC values, several considerations help interpret these results appropriately. Performance in the validation set was comparable to that of the training set, and 10-fold cross-validation demonstrated stable performance across all classification methods. In addition, each of the five metabolites showed strong individual discriminatory ability, which likely contributed to the overall performance of the multivariate model. While these findings reduce concerns regarding overfitting, further evaluation in larger and more diverse external cohorts will be important to fully establish the generalizability of the panel.

Our study has several limitations. First, the absence of a healthy control group limits our ability to fully determine whether the observed metabolic alterations are specific to TB or MAC-PD, or instead represent metabolic changes commonly associated with infection or inflammation. Nevertheless, the primary clinical objective of this study was to address the practical challenge of differentiating TB and MAC-PD patients. Future studies incorporating healthy control cohorts will be important to more clearly delineate metabolic alterations associated with TB and MAC-PD beyond those related to general infection or inflammation. Second, demographic differences such as age, sex, and smoking status may have introduced potential confounding. This is consistent with well-known epidemiologic trends, as NTM-PD predominantly affects older women [43], whereas TB is common in younger men [44]. Nevertheless, subgroup analyses stratified by age, sex, and smoking consistently identified the same five discriminatory metabolites. Moreover, all five metabolites remained significant predictors after covariate adjustment, supporting that the metabolic differences observed between TB and MAC-PD associated lipid alteration rather than demographic differences. Third, although TB and MAC-PD samples were collected in different years and institutions, several measures were implemented to minimize potential batch effects and population-related biases. All serum samples were collected using identical standardized protocols and immediately stored at −80°C, a condition under which global serum metabolite profiles have been shown to remain broadly stable for several years [45]. In addition, all samples were analyzed within a unified analytical workflow using a fully randomized injection order, and comprehensive QC-based normalization was applied to mitigate technical variation and run-order effects. These procedures increase confidence that the metabolic differences observed in this study reflect biological variation associated with disease status rather than batch- or site-related effects. Fourth, as all patients were Korean, external validation in larger and geographically diverse cohorts will be necessary. Finally, concomitant medications, comorbidities, and nutritional status, which could potentially affect systemic metabolic profiles, were not comprehensively adjusted for in this study. Despite these limitations, our findings provide important insights into the metabolic distinctions between TB and MAC-PD and highlight the potential of serum metabolomics as a supportive diagnostic tool.

Currently, the global burden and transmissible nature of TB, together with the rising prevalence of NTM-PD, underscore their importance as major public health challenges. Accordingly, the ability to rapidly and accurately differentiate these conditions carries direct and substantial implications for public health.

## Conclusion

In conclusion, we identified a reproducible five-metabolite serum panel that robustly differentiates TB from MAC-PD at diagnosis. Machine learning-based ROC analyses confirmed its strong discriminatory performance, supporting its role as a supportive biomarker set alongside conventional diagnostic methods. Integration of serum metabolite profiling with clinical and radiographic evaluation may ultimately facilitate earlier and more accurate differentiation of TB and MAC-PD, particularly in patients with negative sputum results or indeterminate culture findings. Such an approach could help prevent unnecessary delays in TB treatment initiation, reduce inappropriate use of anti-TB therapy in NTM-PD, and improve overall patient management.

Abbreviations

| | |
|---|---|
| 2-HG | 2-hydroxyglutaric acid |
| AFB | Acid-fast bacilli |
| All | Allantoin |
| ATP | Adenosine triphosphate |
| AUC | Area under the curve |
| BMI | Body mass index |
| Cer | Ceramide |
| CI | Confidence interval |
| DG | Diacylglycerol |
| DMS | Dimethylsphingosine |
| eLPC | Ether lyso-phosphatidylcholine |
| ePC | Ether phosphatidylcholine |
| ePE | Ether phosphstidylethanolamine |
| FA | Fatty acid |
| FC | Fold change |
| FDR | False discovery rate |
| G3-P | Glycerol 3-phosphate |
| G6-P | Glucose 6-phosphate |
| HIF-1α | Hypoxia-inducible factor-1α |
| HPLC | High-performance liquid chromatography |
| IRB | Institutional Review Boards |
| LPC | Lyso-phosphatidylcholine |
| LPE | Lyso-phosphatidylethanolamine |
| MAC | *Mycobacterium avium* complex |
| MS | Mass spectrometry |
| Mtb | *Mycobacterium tuberculosis* |
| NTM | Nontuberculous mycobacteria |
| PC | Phosphatidylcholine |
| PD | Pulmonary disease |
| PE | Phosphatidylethanolamine |
| PLS-DA | Partial least-squares discriminant analysis |
| PS | Phosphatidylserine |
| QQQ/MS | Triple quadruple mass spectrometer |
| QC | Quality control |
| RBF | Radial basis function |
| ROC | Receiver operating characteristic |
| RSD | Relative standard deviation |
| SE | Standard error |
| SM | Sphingomyelin |
| SPG | Sphinganine |
| SPH | Sphingosine |
| SVM | Support vector machine |
| TB | Tuberculosis |
| UHPLC | Uultrahigh-performance liquid chromatography |
| VIP | Variable importance in projection |

## Author's contributions

Kim KES performed the main experiments and drafted the manuscript. Yim YJ collected clinical samples and contributed to drafting the manuscript. Park JH performed data analysis, validation, and manuscript review. Kwak NK and Jhun BW contributed to sample collection and manuscript review. Kim SY assisted with sample collection. Shin SJ and Yim JJ conceived and supervised the project and contributed to manuscript review and editing. All authors approved the final version of the manuscript.

## Ethical approval

All patient recruitment and the acquisition of informed consent were conducted in adherence to the approved guidelines of the Institutional Review Board (IRB) of Seoul National University Hospital (IRB No. H-2509–085–1676) and Samsung Medical Center (IRB No. SMC-2008–09–016).

## Funding

This work was supported by the National Research Foundation of Korea (NRF) grant funded by the Ministry of Science and ICT (MSIT), South Korea (Grant No. RS-2023–00208115 and RS-2024–00405542). This research was also supported by a grant of the Korea Health Technology R&D Project through the Korea Health Industry Development Institute (KHIDI), funded by the Ministry of Health & Welfare, Republic of Korea (Grant No. RS-2025-02193034).

## Declaration of Competing Interest

The authors declare that they have no known competing financial interests or personal relationships that could have appeared to influence the work reported in this paper.

## Declaration of Generative AI and AI-assisted technologies in the writing process

The authors confirm that generative artificial intelligence tools (ChatGPT 5.2, OpenAI) were used exclusively to assist with language editing and grammatical correction of the manuscript. All scientific content, data analyses, interpretation of findings, and conclusions were independently developed and validated by the authors.

## Acknowledgements

None.

## Appendix A. Supporting information

Supplementary data associated with this article can be found in the online version at doi:10.1016/j.jiph.2026.103162.

## References

[1] World Health Organization. Global Tuberculosis Report 2025 (ISBN 978-92-4-011692-4). Geneva: World Health Organization. Geneva: World Health Organization; 2025. ⟨https://www.who.int/teams/global-programme-on-tuberculosis-and-lung-health/tb-reports/global-tuberculosis-report-2025⟩ (Available:) Accessed December 16, 2025.
[2] Lee H, Kim J, Kim J, Park Y-J. Review of the global burden of tuberculosis in 2023: insights from the WHO Global Tuberculosis Report 2024. Public Health Weekly Report. 2025;18(11):55–69. https://doi.org/10.56786/PHWR.2025.18.11suppl.5
[3] Dahl VN, Mølhave M, Fløe A, van Ingen J, Schön T, Lillebaek T, et al. Global trends of pulmonary infections with nontuberculous mycobacteria: a systematic review. Int J Infect Dis 2022;125:120–31. https://doi.org/10.1016/j.ijid.2022.10.013
[4] Kim J-Y, Kwak N, Yim J-J. The rise in prevalence and related costs of nontuberculous mycobacterial diseases in South Korea, 2010–2021. Open Forum Infect Dis 2022;9(12). https://doi.org/10.1093/ofid/ofac649
[5] Daley CL. *Mycobacterium avium* complex disease. Microbiol Spectr 2017;5(2). https://doi.org/10.1128/microbiolspec.TNMI7-0045-2017
[6] Kim YJ, Kim S, Ham H, Yu S, Choo H-J, Kim H-J, et al. Trend of nontuberculous mycobacteria species and minimal inhibitory concentration in a referral laboratory in Korea from 2013 to 2019. J Infect Public Health 2023. https://doi.org/10.1016/j.jiph.2023.11.028
[7] Lewinsohn DM, Leonard MK, LoBue PA, Cohn DL, Daley CL, Desmond E, et al. Official American Thoracic Society/Infectious Diseases Society of America/Centers for Disease Control and Prevention clinical practice guidelines: diagnosis of tuberculosis in adults and children. Clin Infect Dis 2017;64(2):e1–33. https://doi.org/10.1093/cid/ciw778
[8] Theron G, Venter R, Calligaro G, Smith L, Limberis J, Meldau R, et al. Xpert MTB/RIF results in patients with previous tuberculosis: can we distinguish true from false positive results? Clin Infect Dis 2016;62(8):995–1001. https://doi.org/10.1093/cid/civ1223
[9] Kusumaningrum D, Mertaniasih NM, Soedarsono S, Setiawati R, Pradipta CP. Implication of Negative GeneXpert *Mycobacterium tuberculosis*/Rifampicin Results in Suspected Tuberculosis Patients: A Research Study. Int J Mycobacteriol 2024;13(2):152–7. https://doi.org/10.4103/ijmy.ijmy_100_24
[10] Gopalaswamy R, Shanmugam S, Mondal R, Subbian S. Of tuberculosis and non-tuberculous mycobacterial infections–a comparative analysis of epidemiology, diagnosis and treatment. J Biomed Sci 2020;27(1):1–17. https://doi.org/10.1186/s12929-020-00667-6
[11] Newgard CB. Metabolomics and metabolic diseases: where do we stand? Cell Metab 2017;25(1):43–56. https://doi.org/10.1016/j.cmet.2016.09.018
[12] Yu Y, Jiang X-X, Li J-C. Biomarker discovery for tuberculosis using metabolomics. Front Mol Biosci 2023;10:1099654. https://doi.org/10.3389/fmolb.2023.1099654
[13] Anh NK, Phat NK, Yen NTH, Jayanti RP, Thu VTA, Park YJ, et al. Comprehensive lipid profiles investigation reveals host metabolic and immune alterations during anti-tuberculosis treatment: implications for therapeutic monitoring. Biomed Pharm 2023;158:114187. https://doi.org/10.1016/j.biopha.2022.114187
[14] Kim J, Chae W, Kim J-Y, Yim J-J, Cho J-Y, Kwak N. Metabolomic characteristics of nontuberculous mycobacterial pulmonary disease. J Infect Dis 2024;230(4):797–806. https://doi.org/10.1093/infdis/jiae100
[15] O'Neill LAJ, Kishton RJ, Rathmell J. A guide to immunometabolism for immunologists. Nat Rev Immunol 2016;16(9):553–65. https://doi.org/10.1038/nri.2016.70
[16] Lee M, Lee SY, Bae Y-S. Functional roles of sphingolipids in immunity and their implication in disease. Exp Mol Med 2023;55(6):1110–30. https://doi.org/10.1038/s12276-023-01018-9
[17] van der Meer-Janssen YP, van Galen J, Batenburg JJ, Helms JB. Lipids in host-pathogen interactions: pathogens exploit the complexity of the host cell lipidome. Prog Lipid Res 2010;49(1):1–26. https://doi.org/10.1016/j.plipres.2009.07.003
[18] Griffith DE, Aksamit T, Brown-Elliott BA, Catanzaro A, Daley C, Gordin F, et al. An official ATS/IDSA statement: diagnosis, treatment, and prevention of nontuberculous mycobacterial diseases. Am J Respir Crit Care Med 2007;175(4):367–416. https://doi.org/10.1164/rccm.200604-571ST
[19] Want EJ, O'Maille G, Smith CA, Brandon TR, Uritboonthai W, Qin C, et al. Solvent-dependent metabolite distribution, clustering, and protein extraction for serum profiling with mass spectrometry. Anal Chem 2006;78(3):743–52. https://doi.org/10.1021/ac051312t
[20] Bligh EG, Dyer WJ. A rapid method of total lipid extraction and purification. Can J Biochem Physiol 1959;37(8):911–7. https://doi.org/10.1139/o59-099
[21] Joh J-S, Lee CH, Lee JE, Park Y-K, Bai G-H, Kim E-C, et al. The interval between initiation of anti-tuberculosis treatment in patients with culture-positive pulmonary tuberculosis and receipt of drug-susceptibility test results. J Korean Med Sci 2007;22(1):26–9. https://doi.org/10.3346/jkms.2007.22.1.26
[22] Ryu YJ, Koh WJ, Daley CL. Diagnosis and treatment of nontuberculous mycobacterial lung disease: clinicians' perspectives. Tube Respir Dis (Seoul) 2016;79(2):74–84. https://doi.org/10.4046/trd.2016.79.2.74
[23] Bae J, Park S-B, Kim J-H, Kang MR, Lee KE, Kim S, et al. Comparison of the three molecular diagnostic assays for molecular identification of *Mycobacterium tuberculosis* and nontuberculous mycobacteria species in sputum samples. Biomed Sci Lett 2020;26(3):170–8. https://doi.org/10.15616/BSL.2020.26.3.170
[24] Anh NK, Phat NK, Thu NQ, Tien NTN, Eunsu C, Kim H-S, et al. Discovery of urinary biosignatures for tuberculosis and nontuberculous mycobacteria classification using metabolomics and machine learning. Sci Rep 2024;14(1):15312. https://doi.org/10.1038/s41598-024-66113-x
[25] Naito M, Takeda Y, Edahiro R, Shirai Y, Enomoto T, Nakayama M, et al. NHERF2 as a novel biomarker for distinguishing MAC pulmonary disease from tuberculosis based on proteome analysis of serum extracellular vesicles. Int J Mol Sci 2025;26(3):1155. https://doi.org/10.3390/ijms26031155
[26] Van den Bossche J, O'Neill LA, Menon D. Macrophage immunometabolism: where are we (going)? Trends Immunol 2017;38(6):395–406. https://doi.org/10.1016/j.it.2017.03.001
[27] Ganeshan K, Chawla A. Metabolic regulation of immune responses. Annu Rev Immunol 2014;32:609–34. https://doi.org/10.1146/annurev-immunol-032713-120236
[28] Macintyre AN, Rathmell JC. Activated lymphocytes as a metabolic model for carcinogenesis. Cancer Metab 2013;1:1–12. https://doi.org/10.1186/2049-3002-1-5
[29] Park J-H, Shim D, Kim KES, Lee W, Shin SJ. Understanding metabolic regulation between host and pathogens: new opportunities for the development of improved therapeutic strategies against *Mycobacterium tuberculosis* infection. Front Cell Infect Microbiol 2021;11:635335. https://doi.org/10.3389/fcimb.2021.635335
[30] Intlekofer AM, Dematteo RG, Venneti S, Finley LW, Lu C, Judkins AR, et al. Hypoxia induces production of L-2-hydroxyglutarate. Cell Metab 2015;22(2):304–11. https://doi.org/10.1016/j.cmet.2015.06.023
[31] Fathi AT, Sadrzadeh H, Comander AH, Higgins MJ, Bardia A, Perry A, et al. Isocitrate dehydrogenase 1 (IDH1) mutation in breast adenocarcinoma is associated with elevated levels of serum and urine 2-hydroxyglutarate. oncologist 2014;19(6):602–7. https://doi.org/10.1634/theoncologist.2013-0417
[32] Wu Y, Liu Y, Gulbins E, Grassmé H. The anti-infectious role of sphingosine in microbial diseases. Cells 2021;10(5):1105. https://doi.org/10.3390/cells10051105
[33] Futerman AH, Hannun YA. The complex life of simple sphingolipids. EMBO Rep 2004;5(8):777–82. https://doi.org/10.1038/sj.embor.7400208
[34] Schnitker F, Liu Y, Keitsch S, Soddemann M, Verhasselt HL, Kehrmann J, et al. Reduced Sphingosine in Cystic Fibrosis Increases Susceptibility to *Mycobacterium abscessus* Infections. Int J Mol Sci 2023;24(18):14004. https://doi.org/10.3390/ijms241814004
[35] Aloulou A., Rahier R., Arhab Y., Noiriel A., Abousalham A., Phospholipases: an overview. Lipases and Phospholipases: Methods and Protocols, 2018. p. 69-105. https://doi.org/10.1007/978-1-4939-8672-9_3.
[36] Tan ST, Ramesh T, Toh XR, Nguyen LN. Emerging roles of lysophospholipids in health and disease. Prog Lipid Res 2020;80:101068. https://doi.org/10.1016/j.plipres.2020.101068
[37] Furse S, De Kroon AI. Phosphatidylcholine's functions beyond that of a membrane brick. Mol Membr Biol 2015;32(4):117–9. https://doi.org/10.3109/09687688.2015.1066894

[38] Bernhard W. Lung surfactant: Function and composition in the context of development and respiratory physiology. Ann AnatAnat Anz 2016;208:146–50. https://doi.org/10.1016/j.aanat.2016.08.003
[39] Chimote G, Banerjee R. Lung surfactant dysfunction in tuberculosis: effect of mycobacterial tubercular lipids on dipalmitoylphosphatidylcholine surface activity. Colloids Surf B Biointerfaces 2005;45(3-4):215–23. https://doi.org/10.1016/j.colsurfb.2005.08.014
[40] Chen J-X, Han Y-S, Zhang S-Q, Li Z-B, Chen J, Yi W-J, et al. Novel therapeutic evaluation biomarkers of lipid metabolism targets in uncomplicated pulmonary tuberculosis patients. Signal Transduct Target Ther 2021;6(1):22. https://doi.org/10.1038/s41392-020-00427-w
[41] Shivakoti R, Newman JW, Hanna LE, Queiroz AT, Borkowski K, Gupte AN, et al. Host lipidome and tuberculosis treatment failure. Eur Respir J 2022;59(1). https://doi.org/10.1183/13993003.04532-2020
[42] Gray RM, Hunt DM, Silva dos Santos M, Liu J, Agapova A, Rodgers A, et al. *Mycobacterium tuberculosis* overcomes phosphate starvation by extensively remodelling its lipidome with phosphorus-free lipids. Nat Commun 2025. https://doi.org/10.1038/s41467-025-66437-w
[43] Lee H, Myung W, Lee E-M, Kim H, Jhun BW. Mortality and prognostic factors of nontuberculous mycobacterial infection in Korea: a population-based comparative study. Clin Infect Dis 2021;72(10):e610–9. https://doi.org/10.1093/cid/ciaa1381
[44] Min J, Kim HW, Kim JS. Tuberculosis: Republic of Korea, 2021. Tuberc Respir Dis 2023;86(1):67. https://doi.org/10.4046/trd.2022.0111
[45] Wagner-Golbs A, Neuber S, Kamlage B, Christiansen N, Bethan B, Rennefahrt U, et al. Effects of long-term storage at− 80C on the human plasma metabolome. Metabolites 2019;9(5):99. https://doi.org/10.3390/metabo9050099